The boundary conditions (eqns. 4 and 6) are then reduced to a matrix form. The result is

$$[Z][I] = [V] \tag{7}$$

$$[Z] = \begin{bmatrix} [Z^{I}] & [0] \\ [0] & [Z^{II}] \end{bmatrix}$$

$$[I] = \begin{bmatrix} \begin{bmatrix} A^{I} \\ B^{I} \end{bmatrix} \\ \begin{bmatrix} A^{II} \\ B^{II} \end{bmatrix} \end{bmatrix} \tag{8}$$

$$[V] = \begin{bmatrix} [0] \\ [V^{II}] \end{bmatrix}$$

where (A^{I}, B^{I}) and (A^{II}, B^{II}) are the expansion coefficients of E_z^{di} on Γ_1 and on Γ_2, respectively, and $[V^{II}]$ is involved in E^{inc}.

By means of the point-matching method (PMM), unknown current vector $[I]$ can be solved in a straightforward manner; thereby the field E^{di} in region II is obtained.

Applying the boundary condition (eqn. 5*a*), the scattering field E^{sc} can be obtained from the solution to E^{di} and given E^{inc}.

$$\sum_{i=1}^{N^{I}} A_i[H_0^{(2)}(k_1\rho_i^{I}) + B_i H_0^{(1)}(k_1\rho_i^{I})] = E_z^{inc} + \sum_{i=1}^{N^{II}} S_i H_0^{(2)}(k_0\rho_i^{II}) \tag{9}$$

Therefore the problem of the electromagnetic scattering from a dielectric coated cylinder can be analysed.

Numerical results: To check the accuracy of the suggested method, some cases are considered for which exact solutions are known. The suggested solution yields very accurate numerical approximations to the scattering cross-section. Figs. 3 and 4 show the case of a circular cylinder of $k_0 a_1 = k_0 b_1 = 1{\cdot}57$, $k_0 a_2 = k_0 b_2 = 6{\cdot}28$, $\varepsilon_r = 2{\cdot}5 + j1{\cdot}0$, $\mu_r = 1{\cdot}0$, $a = 90°$, and elliptic cylinders of $k_0 a_1 = 5{\cdot}024$, $k_0 b_1 = 1{\cdot}256$, $a_2/a_1 = 1.\ 25$, $b_2/b_1 = 2{\cdot}2$, $\varepsilon_r = 2{\cdot}5$, $\mu_r = 1{\cdot}0$, $a = 90°$, $\theta = a - 90°$. These results show that this method may also be applied to various geometries of conducting cylinders with electrically larger smooth profile coated by a dielectric and the results are in good agreement with those in Reference 4 using the classical method.

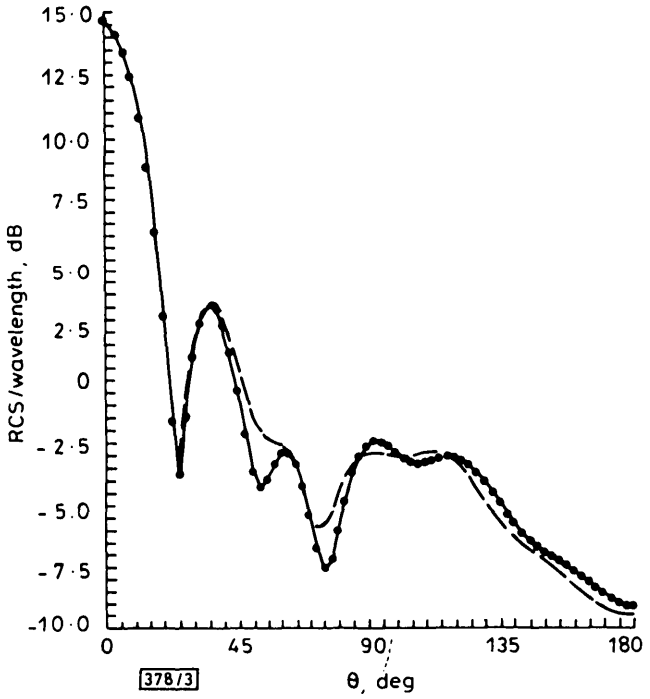

Fig. 3 *Bistation RCS of dielectric coated concentrically circular cylinder*

——— $N = 24$ solution
– – – – $N = 22$ solution
····· exact solution

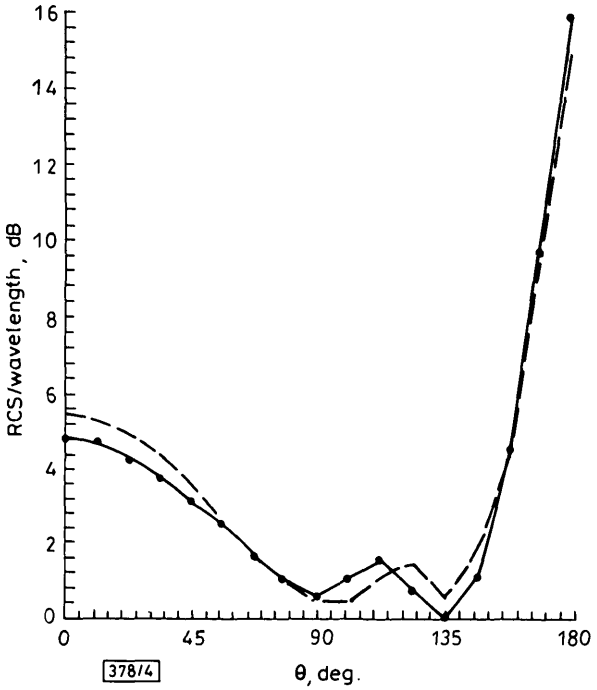

Fig. 4 *Bistation RCS of dielectric coated confocally elliptic cylinder*

——— $N = 24$ solution
– – – – $N = 16$ solution
····· exact solution

Obviously, the case of TE incidence can also be analysed in a similar way.

18th March 1993

Z.-N. Chen (*Department of Radio Engineering, Communication Engineering Institute, 2 Biao-Ying, Nanjing, 210016, People's Republic of China*)

W.-X. Zhang (*Department of Radio Engineering, Southeast University, 2 Si-Pai-Lou, Nanjing, 210018, People's Republic of China*)

References

1 LEVIATAN, Y., and BOAG, A.: 'Analysis of electromagnetic scattering from dielectric cylinders using a multifilament current model', *IEEE Trans.*, 1987, **AP-35**, pp. 1119–1127

2 KRIEGSMANN, G. A., TAFLOVE, A., and UMASHANKAR, K. R.: 'A new formulation of electromagnetic wave scattering using an on-surface radiation boundary condition approach', *IEEE Trans.*, 1987, **AP-35**, pp. 153–161

3 CHEN, Z. N., and ZHANG, W. X.: 'Application of OSRC operator of 3rd order to electromagnetic scattering from conducting or dielectric cylinder', *Electron. Lett.*, 1991, **27**, pp. 806–808

4 RAGHED, H. A., SHAFAI, L., and HAMID, M.: 'Plane wave scattering by a conducting elliptic cylinder coated by a nonconfocal dielectric', *IEEE Trans.*, 1991, **AP-39**, pp. 218–223

WIDE SPECTRUM SINGLE QUANTUM WELL SUPERLUMINESCENT DIODES AT 0·8μm WITH BENT OPTICAL WAVEGUIDE

A. T. Semenov, V. R. Shidlovski and S. A. Safin

Indexing terms: Diodes, Light emitting diodes, Semiconductor devices and materials

An AlGaAs quantum well superluminescent diodes (SLDs) with 68 nm spectral width at 5 mW output power have been developed. With 4 μm mesa stripe angled at 7° with respect to the output facet, the spectral ripple was less than 10% for uncoated devices.

Introduction: Superluminescent diodes (SLDs) are optimum light sources for optical sensors and short and medium dis-

tance fibre optic links. It has been shown that the use of a quantum well (QW) structure in SLDs allows the spectral bandwidth of devices to be widened with respect to that of bulk SLDs. Spectral bandwidths of 54 nm [1] and 170 nm [2] have been realised at 800 and 1500 nm in QW SLDs, respectively.

In Reference 2, a wide spectrum was obtained due to amplification of intrinsic spontaneous emission by $n = 1$ and $n = 2$ transitions simultaneously. It was shown in Reference 3 that the full width of the gain spectrum of the AlGaAs/GaAs QWS at $n = 1$ and $n = 2$ transitions may be around 100 nm. Nevertheless simultaneous amplification of intrinsic spontaneous emission by $n = 1$ and $n = 2$ QW transitions has not been used to date to widen the 800 nm-band SLDs spectrum.

We report the development of '($n = 1, 2$) transition' AlGaAs SCH-QW SLDs.

SLD structure: SLDs were based on an MOCVD-grown separate confinement AlGaAs heterostructure with step-index waveguide (total thickness 0·25 μm) and 8 nm-thick active layer. A deep mesa 4 μm-wide was then etched on-wafer to provide lateral confinement. To prevent optical feedback in the structure, the mesa ridge was bent near the outpur facet of the device to obtain an angle of 7° with respect to the normal to the facet. The total length of the bent part of the mesa was 250 μm. The rear side of the device ridge was perpendicular to the facet. A schematic diagram of the top view of the device is shown on Fig. 1. No facet coatings were used.

To obtain stable simultaneous amplification of spontaneous emission by $n = 1$ and $n = 2$ transitions it is very important to optimise the total length of the SLDs. It is known [4] that the gain at the $n = 1$ transition flattens with an increase in current (carrier) density and for some fixed current it becomes equal to the gain at $n = 2$ transition, as schematically shown in Fig. 2. For high currents the $n = 2$ gain becomes higher than that of $n = 1$.

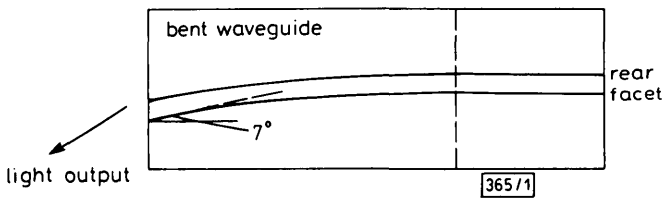

Fig. 1 *Top view of SLDs*

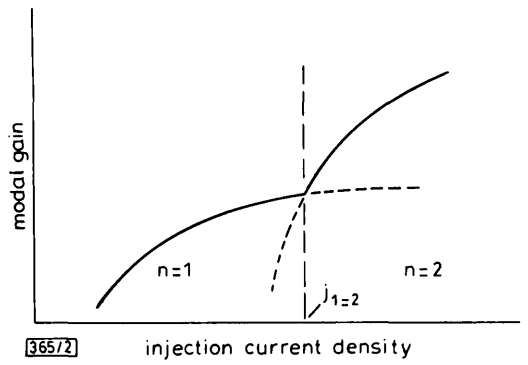

Fig. 2 *Modal gain against current density for QW structures*

This means that if the current density is less than $J_{1=2}$ then spontaneous emission amplified by the $n = 1$ transition dominates in the output spectrum. In turn, if the current density is more than $J_{1=2}$ then spontaneous emission amplified by the $n = 2$ transition dominates. Therefore the length of the device must be optimised to obtain maximum output power and maximum spectral bandwidth at current densities around the point $J_{1=2}$ in Fig. 2.

SLD output characteristics: Our experiments show that for our structures, the optimum length of the SLDs was around 550 μm. Figs. 3 and 4 show the light-current characteristic and output spectrum at different pumping levels for a 550 μm SLD at 20°C. It is seen that for currents more than 230 mA, the SLD emits stably at the $n = 1$ and $n = 2$ transitions simultaneously. For SLDs less than 450 μm, the spectrum (for appropriate output power, 1 mW and more) was concentrated at an $n = 2$ related wavelength. For long (more than 600 μm)

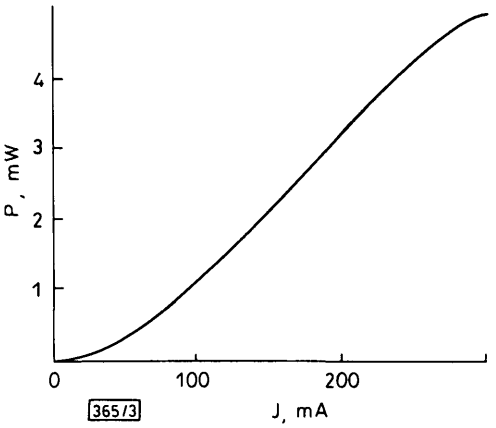

Fig. 3 *Light-current characteristic of 550 μm SLD*

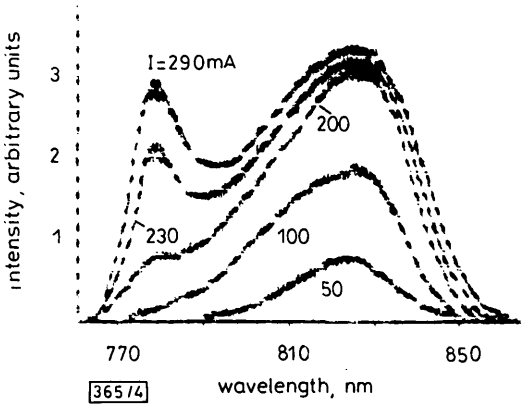

Fig. 4 *550 μm SLD spectra at different injection currents*

devices, the spectrum was concentrated around an $n = 1$ related wavelength at injection currents less then 300 mA. In such long devices we did not obtain an amplified $n = 2$ related spectrum. For short (<450 μm) and long (>600 μm) devices, the typical spectral bandwidth did not exceed 30 nm for more than 1 mW output power.

It is seen from Fig. 4 that the maximum spectral width $\delta\lambda$ is nearly 68 nm for a 550 μm device. The corresponding coherence length of the output beam, calculated as $\lambda^2/\delta\lambda$, is 9·2 μm.

It is also seen from Fig. 4 that an angled mesa allows the spectral ripple to be reduced to 7% without any antireflection coatings on the crystal facet.

For practical applications, coupling of SLD light to optical fibres is important. With 4 μm core diameter, a coupling efficiency of a tapered microlensed fibre of 17% was obtained in our experiments.

It is known that double-path amplification of spontaneous emission is very attractive for increasing the output power of an SLD [5]. In the QW SLDs presented here, only 30% of light at the rear facet was then 'double-path amplified' and 70% of the rear facet output was lost. A high reflectivity coating on the rear facet together with an antireflection coating on the output facet may lead to a further increase in the SLD output power.

Conclusions: Single quantum well SLDs with 68 nm spectral bandwidth and 5 mW CW output power at 0·8 μm have been developed. Through the use of a curved active waveguide and angled mesa ridge, the spectral ripple was reduced to 7% without any coating of the cleaved facets.

17 March 1993

A. T. Semenov, V. R. Shidlovski and S. A. Safin (*Superlum Ltd., PO Box 73, E-538 Moscow 111538, Russia*)

References

1 CHEN, T. R., ENG, L., ZHUANG, Y. H., YARIV, A., KWONG, N. S., and CHEN, P. C.: 'Quantum-well superluminescent diode with very wide emission spectrum', *Appl. Phys. Lett.*, 1990, **56**, pp. 1345–1346

2 KONDO, S., YASAKA, H., NOGUCHI, Y., MAGARI, K., SUGO, M., and KIKAMI, O.: 'Very wide spectrum multiquantum well superluminescent diode at 1·5 μm', *Electron. Lett.*, 1992, **28**, pp. 132–133
3 MECHIYS, D., MITTELSTEIN, M., YARIV, A., SARFATY, R., and UNGAR, J.: 'Optimized Fabry-Perot (AlGa)As QW lasers tunable over 105 nm', *Electron. Lett.*, 1989, **25**, pp. 143–145
4 ARAKAWA, Y., and YARIV, A.: 'Quantum well lasers—gain, spectra, dynamics', *IEEE J. Quantum Electron*, 1986, **QE-56**, pp. 1887–1899.
5 LIN, C.-F.: 'Superluminescent diodes with angled facet etched by chemically assisted ion beam etching', *Electron Lett.*, 1991, **27**, pp. 968–970

QUADRATIC PHASE INTERPOLATION FOR VOICED SPEECH SYNTHESIS IN MBE MODEL

H. Yang, S.-N. Koh and P. Sivaprakasapillai

Indexing term: Speech synthesis

A new phase unwrapping algorithm for phase interpolation in voiced speech synthesis is proposed. Computer simulation results show that the new algorithm outperforms the original phase unwrapping method proposed by Griffin and Lim in terms of the number of instances of wrongly unwrapped phase.

Introduction: A speech signal is to a great extent quasi-stationary and therefore it is usually analysed on a short time frame basis with the assumption that the signal characteristics are stationary within each analysis frame. Parameters such as linear predictive coefficients and pitch period are estimated for each frame. Usually, these parameters are not continuous from frame to frame. To obtain high quality synthesised speech, some of these parameters are made to vary from sample to sample within each individual frame during synthesis. The variation is performed using an interpolation process which matches the parameters between adjacent frames.

In the multiband excitation (MBE) model [1, 2], harmonic frequencies and phases are smoothed under certain conditions in order to obtain a continuous waveform in the time domain. Griffin and Lim [2] suggested the representation of the instantaneous frequency as the sum of the linearly interpolated value between the measured frequencies of two neighbouring frames, and a frequency deviation term, which was a constant within a frame. We note that the result of such a representation is that the phase becomes a quadratic function of time. In this Letter, a new phase unwrapping method is proposed. It is compared with the method which minimises the absolute value (AFD) of the frequency deviation term. Our simulation results show that this new method, when used for quadratic interpolation in voiced speech synthesis with the MBE model, is better than the method that minimises the AFD term.

Phase interpolation based on quadratic polynomial: Griffin and Lim [2] suggested an expression for the instantaneous frequency, which may be written in the form

$$F^{[k]}(t) = f^{[k]} + (f^{[k-1]} - f^{[k]})\frac{S-t}{S} + \Delta f^{[k]} \tag{1}$$

where $f^{[k-1]}, f^{[k]}$ are the measured frequencies of the previous and current frame, S is the frame length, and $\Delta f^{[k]}$ is a frequency deviation to be discussed below. In this expression, the instantaneous frequency $F^{[k]}(t)$ is a linear function of time t. We then find that the phase, which is the integral of $F^{[k]}(t)$ with respect to t, will be a quadratic function of t and will be given by

$$\theta^{[k]}(t) = \frac{1}{2S}(f^{[k]} - f^{[k-1]})t^2 + (f^{[k+1]} + \Delta f^{[k]})t + \Phi_0^{[k]} \tag{2}$$

where $\Phi_0^{[k]}$ is the initial phase of the current frame. To smooth the phase function at the frame boundaries, the phase at the beginning of the current frame should satisfy

$$\theta^{[k-1]}(S) = \theta^{[k]}(0) + 2\pi M^{[k]} \tag{3}$$

$2\pi M^{[k]}$ is used for phase unwrapping (integer $M^{[k]}$ will be examined in the following Section). The measured parameters are used to set the phase at the end of the two frames in accordance with the following equations.

$$\theta^{[k-1]}(S) = S \cdot f^{[k-1]} + \varphi^{[k-1]} \tag{4}$$

$$\theta^{[k]}(S) = S \cdot f^{[k]} + \varphi^{[k]} \tag{5}$$

Combining $\theta^{[k]}(0) = \Phi_0^{[k]}$, which is the direct result of eqn. 2 at $t = 0$, with eqns. 3 and 4, the initial phase of the current frame can be expressed in terms of the measured parameters $f^{[k-1]}$ and $\varphi^{[k-1]}$ as

$$\Phi_0^{[k]} = S \cdot f^{[k-1]} + \varphi^{[k-1]} - 2\pi M^{[k]} \tag{6}$$

Substituting for $\theta^{[k]}(S)$ from eqn. 5 in eqn. 2 at $t = S$ and substituting for $\Phi_0^{[k]}$ from eqn. 6, the frequency deviation of the current frame is given by

$$\Delta f^{[k]} = \tfrac{1}{2}(f^{[k]} - 3f^{[k-1]}) + \frac{1}{S}(\varphi^{[k]} - \varphi^{[k-1]} + 2\pi M^{[k]}) \tag{7}$$

By substituting eqns. 6 and 7 into eqn. 2, the phase function of the current frame becomes

$$\begin{aligned}\theta^{[k]}(t) = {} & \frac{f^{[k]} - f^{[k-1]}}{2S}t^2 \\ & + \left(\frac{f^{[k]} - f^{[k-1]}}{2} + \frac{\varphi^{[k]} - \varphi^{[k-1]} + 2\pi M^{[k]}}{S}\right)t \\ & + (S \cdot f^{[k-1]} + \varphi^{[k-1]} - 2\pi M^{[k]})\end{aligned} \tag{8}$$

The key problem is to choose $M^{[k]}$, for the purpose of phase unwrapping. Two unwrapping algorithms, designated as *Quad1* and *Quad2*, are studied in the following Section. Simulation results based on the two algorithms are presented in the 'Simulation results' Section.

Phase unwrapping algorighms for phase interpolation:

(i) *Quad1:* This algorithm involves the minimisation of the AFD term, i.e. $|\Delta f^{[k]}|$. Defining a new term $X^{[k]}$ by the equation

$$X^{[k]} = \frac{S}{4\pi}(f^{[k]} - 3f^{[k-1]}) + \frac{1}{2\pi}(\varphi^{[k]} - \varphi^{[k-1]}) \tag{9}$$

we may rewrite eqn. 7 as

$$\Delta f^{[k]} = \frac{2\pi}{S}(X^{[k]} + M^{[k]}) \tag{10}$$

Suppose $X^{[k]} = X_I + X_F$, where X_I is the integer nearest to $X^{[k]}$ and $-0{\cdot}5 < X_F \leq 0{\cdot}5$. We then have for minimum $|\Delta f^{[k]}|$,

$$M^{[k]} = -X_I \tag{11}$$

(ii) *Quad2:* This second algorithm is based on the argument that the interpolated instantaneous frequency $F^{[k]}(t)$ should deviate as little as possible from the measured average frequency $f^{[k]}$ for the whole frame. Therefore, $M^{[k]}$ is chosen so as to minimise $|T^{[k]}|$, which is expressed as

$$T^{[k]} = \int_0^S (F^{[k]}(t) - f^{[k]})\,dt \tag{12}$$